



Orbital Debris

Quarterly News

Volume 27, Issue 3
August 2023

Inside...

DAS Release.....	2
MEO Releases New Example Library.....	3
Updated Flux Interpolation in ORDEM.....	5
Evolution of Major Debris Clouds in LEO.....	7
ODPO Receives the 2022 Agency Group Achievement Honor Award.....	12
Upcoming Meetings.....	12
Orbital Debris Environment Plot.....	13
Space Missions and Satellite Box Score.....	14

IOC II Announces Program and Venue



The Second International Orbital Debris Conference (IOC II) will convene December 4–7, 2023 in Sugar Land, Texas. The conference goal is to highlight orbital debris research activities in the United States and to foster collaborations with the international community. The four-day conference will cover all aspects of orbital debris research, operations and mission support, environment management, and other related

activities. The deadline for the submission of abstracts closed on April 6, 2023, after an extension. The paper submission deadline is November 2, 2023. The IOC II program and abstracts are now available online. Hotel, registration, and additional information will be available at <https://www.hou.usra.edu/meetings/orbitaldebris2023/>. ♦

Continuing Development of ISO Debris Mitigation Standards

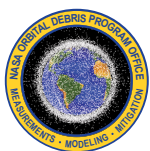
J. OPIELA

The International Organization for Standardization (ISO) is a global source of commercial standards. The ISO's members are the national standards bodies of countries from around the world, such as the American National Standards Institute (ANSI) representing the United States. Composed of delegates appointed by the national standards bodies, the ISO technical working groups

draft, maintain, and update ISO standards, specifications, and reports.

These voluntary standards aim to share knowledge, support innovation, and provide solutions to a wide range of business and industrial endeavors. Through agreements with ISO, some organizations and regulatory bodies use ISO standards as the basis for their own standards.

continued on page 2



A publication of the
NASA Orbital Debris
Program Office (ODPO)

ISO Update

continued from page 1

ISO published its top-level orbital debris mitigation standard, “ISO Standard 24113, Space systems – Space debris mitigation requirements,” for the first time in 2010, quickly followed by a minor revision in 2011. The goal of the standard is to reduce the growth of orbital debris in near-Earth space by applying mitigation requirements to robotic spacecraft and launch vehicle orbital stages from design through operations and disposal. This standard is supplemented by several lower-level implementation standards and technical reports.

The 2019 paper by Stokes, *et al.*, describes the background, structure, and content of the space debris mitigation standards published by the ISO [1]. Among other things, the paper describes the changes made in the third edition of ISO 24113, published earlier in 2019. The revised standard added new requirements and limits to mission-related debris, to the avoidance of collision with known orbital objects, and to the execution and probability of successful post-mission disposal.

The reentry casualty expectation threshold of 10^{-4} (“one in ten thousand”) was introduced in an informative note (*i.e.*, not a requirement). The paper notes that ISO debris standards will continue to evolve considering the great changes taking place in the space industry and in the orbital environment. Soon after publication of the third edition, the ISO Orbital Debris Working Group, referred to in the ISO hierarchy as ISO/TC20/SC14/

WG7, began discussion of issues of primary importance for the next edition.

Debate within the ISO working group separated the issues into two categories: “fast-track” issues with broad general agreement, limiting discussion to the specific wording within the standard; and “regular-track” issues likely to require extensive data collection and debate. The fast-track issues were pushed through an accelerated schedule for the fourth edition of ISO 24113, published in May 2023 [2]. Among these many items, three that were previously optional, informative, or external to the ISO Standard, are now mandatory: 1) assessment of the probability (without a required threshold) of meteoroid or orbital debris impact preventing successful post-mission disposal, 2) assessment of ground hazards from reentering objects, and 3) the qualitative requirement that the expected number of casualties from a reentry be less than 10^{-4} .

The term “casualty risk” is replaced by the more precise “expected number of casualties.” New informative notes to requirements on disposal of objects in low Earth orbit emphasize that the 25-year disposal lifetime is an upper limit, and that the goal is post-mission orbital lifetimes significantly shorter than 25 years. In a similar vein, the phrase “timely manner” was added to the passivation requirements to emphasize that passivation should occur as soon as an energetic system is no longer needed.

continued on page 3

Debris Assessment Software 3.2.5 Release

The NASA Orbital Debris Program Office has released version 3.2.5 of the Debris Assessment Software (DAS), replacing the prior April 2023 release of DAS 3.2.4. The updated version provides data that can verify compliance of a spacecraft, upper stage, and/or payload with NASA’s requirements for limiting debris generation, spacecraft vulnerability, post-mission disposal, and reentry safety.

This release incorporates a fix to the Requirement 4.5-1 assessment of large-object collision risk. The previous version 3.2.4 incorrectly read in ORDEM output files, which resulted in an erroneously higher flux value than expected.

Users who have already completed the software request process for earlier versions of DAS 3.x do not need to reapply for DAS 3.2.5. Simply go to your existing account on the NASA Software portal and download the latest installer. Due to file size limits, the installer has been split into several .zip archive files: the main installer and five separate files containing debris environment data. Users must download the main installer (which includes the debris environment for years 2016 to 2030) and additional environment files required to assess mission years beyond 2030.

Approval for DAS is on a per project basis; approval encompasses activities and personnel working within the project scope identified in the application. For new users, DAS is available for download, pending an approved application submission, via the NASA Software Catalog. To begin the process, click on the Request Software button at <https://software.nasa.gov/software/MS-26690-1>.

ISO Update

continued from page 2

Other modifications in the fourth edition include several clarifying and informative notes and minor editorial changes.

With publication of the fourth edition, the ISO Orbital Debris working group now begins preparations for the “regular-track” fifth edition. The group meets semi-annually, coordinating with the Operations and Ground Support Working Group (ISO/TC20/SC14/WG3), and continues discussions via email. At the recent week-long spring meeting, hosted by the Brazilian Association of Technical Standards (ABNT) and held at the Parque Tecnológico de São José dos Campos, project leads briefed delegates on the status of their documents.

Delegates from industry and government agencies spent one day reviewing both new and previously deferred comments on ISO 24113 and solicited new ideas for future discussion. These topics include mandatory check-out orbits, collision avoidance, higher reliability thresholds, a five-year disposal rule, and high-altitude disposal orbits. Another topic is the possible application of debris mitigation requirements to non-Earth orbits. Some

topics have a growing body of data (supportive or otherwise) to inform discussion, while others may need further study.

ISO does not carry out scientific studies but relies on the knowledge brought by the delegates. The drafting process is guided by inputs and publications from industry, space agencies and regulatory bodies, and, most importantly, the Inter-Agency Space Debris Coordination Committee. To be relevant and effective, the world’s standards organizations must keep pace with the knowledge of, use of, and effects on the space environment.

References

1. Stokes, Hedley, *et al.* “Evolution of ISO’s Space Debris Mitigation Standards,” First International Orbital Debris Conference (IOC), (December 2019).
2. ISO 24113:2023 *Space systems — Space debris mitigation requirements*, International Organization for Standardization, Geneva, Switzerland, (2023). ♦

PROJECT REVIEW

Meteoroid Environment Office Releases New Environment Example Library

A. MOORHEAD

NASA’s Meteoroid Engineering Model (MEM) is used to generate a description of the meteoroid environment specific to a user’s spacecraft trajectory [1]. The environment is described by a set of files that provide not only the meteoroid flux, but also the corresponding distributions of the meteoroids’ direction of motion, speed, and bulk density. These output files are designed to be used in conjunction with a risk assessment code such as Bumper [2], but users can also opt to perform a custom damage assessment; see Equation 4 of reference [3].

Users are likely to make simultaneous use of both MEM and the Orbital Debris Engineering Model (ORDEM); however, unlike orbital debris, which is confined to Earth orbit, meteoroids are present throughout the solar system [4, 5]. As a result, MEM cannot assume that the user’s spacecraft is orbiting the Earth and must instead accept a wide range of possible trajectories (MEM’s limitations are specified in [3]). Furthermore, meteoroid density follows a continuous distribution that is unlike the distinct density classes populated by human-made orbital debris [1]. Thus, MEM and ORDEM differ both in their required inputs and in the structure of their output, increasing the time a new user must spend learning to use the two models.

NASA’s Meteoroid Environment Office (MEO) has released an [online library](#) of sample MEM runs designed to assist and orient the new MEM user. This library includes at least one publicly available example trajectory orbiting every major body in

the inner solar system as well as an Earth-Mars transfer trajectory (see table). For each example, we provide the trajectory file, visualizations of all MEM outputs, and a list of run options that the user can use to replicate our examples. These examples may serve as useful test cases for fresh MEM installations and/or references upon which users can build to create their own customized runs.

continued on page 4

Table. List of spacecraft or generic trajectories included in the MEM example library, sorted by the body that they orbit or lie nearest to (left column).

Nearest Body	Spacecraft or Trajectory
Earth	International Space Station (ISS) Aqua Geostationary Operational Environmental Satellites (GOES)-14 James Webb Space Telescope (JWST)
Moon	Lunar Atmosphere and Dust Environment Explorer (LADEE) Near-rectilinear halo orbit (NRHO)
Mercury	Mercury Surface, Space Environment, Geochemistry, and Ranging (MESSENGER)
Venus	Venus Express
Mars	Mars Reconnaissance Orbiter (MRO) Mars Atmosphere and Volatile Evolution (MAVEN)
Sun	MAVEN (transfer trajectory)

MEO Release

continued from page 3

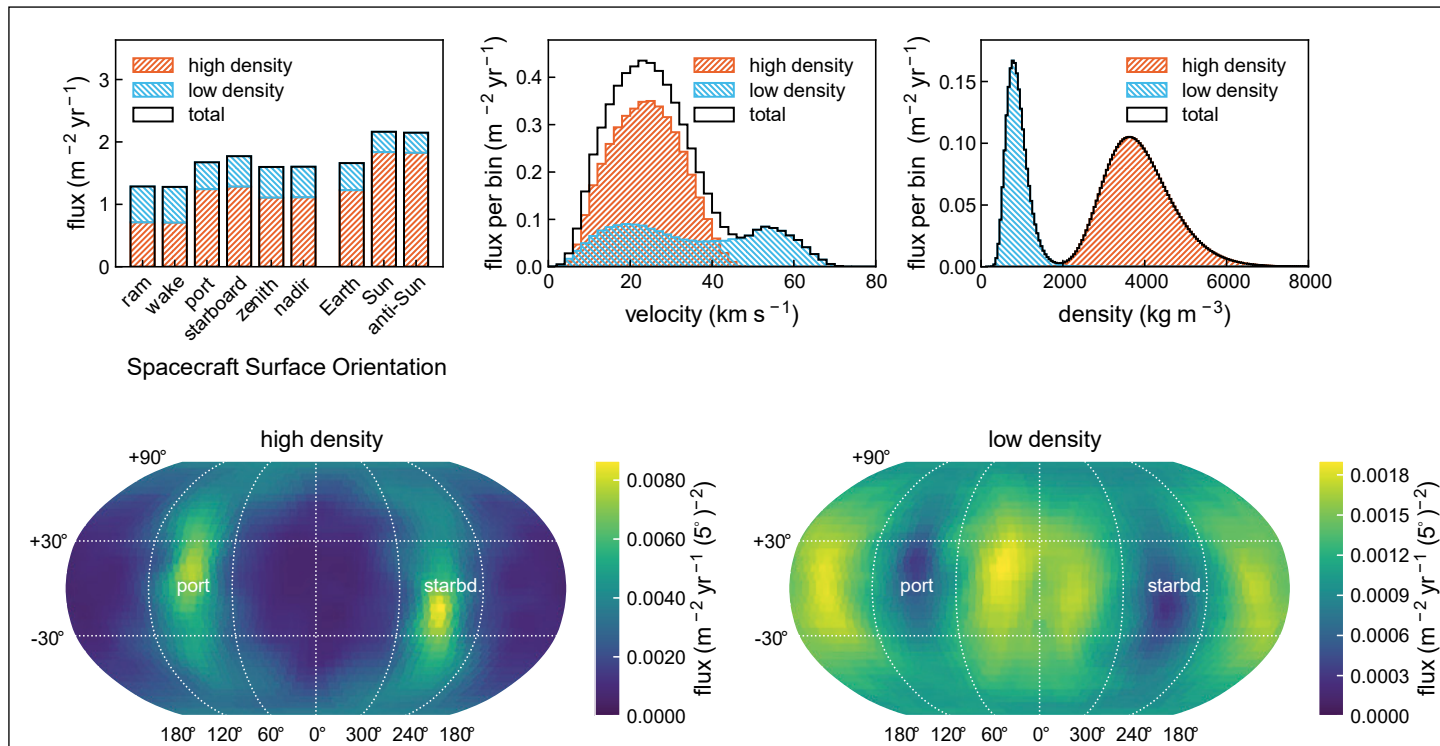


Figure 1. A sample set of visualizations of the microgram-or-larger meteoroid flux encountered along an NRHO trajectory.

Visualizations and run options correspond to [MEM 3](#), but the trajectory files for Earth- and Moon-orbiting spacecraft can also be used with earlier versions of MEM.

Each set of visualizations includes both plots of the input trajectory and of the MEM outputs. Figure 1 presents the meteoroid flux encountered along the near-rectilinear halo orbit (NRHO) trajectory [6]. The first plot displays the flux on surfaces with different orientations; for instance, the column labeled “ram” shows the flux on a surface facing in the direction of the spacecraft’s motion. The top-center plot displays the speed

distribution relative to the spacecraft, and the top-right plot displays the density distribution. All three plots show flux totals as well as fluxes corresponding to meteoroid populations with high and low bulk densities (with modes of 3792 and 857 $kg m^{-3}$, respectively; see reference [7]).

The second row presents the apparent directionality of meteoroids in each density group. These directional maps are aligned with the spacecraft’s direction of motion; that is, the angular coordinate (0°, 0°) points along the spacecraft’s velocity vector.

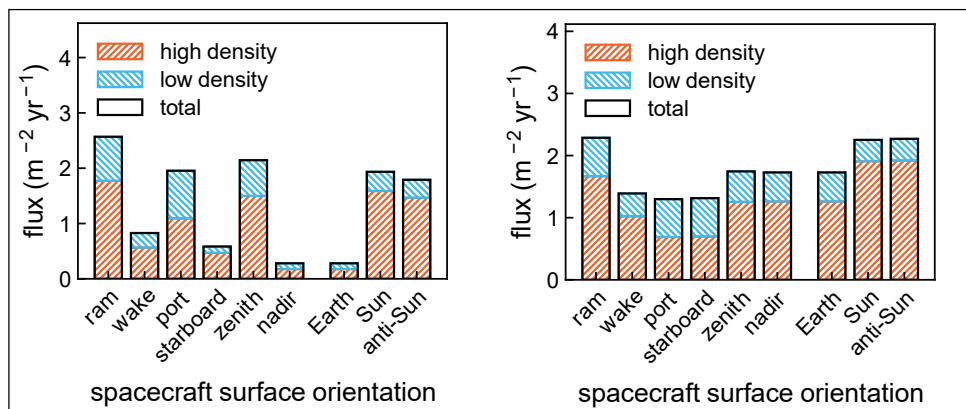


Figure 2. (Left) The flux of microgram-or-larger meteoroids on the spacecraft Aqua for surfaces with different orientations. Note that the flux on the nadir- or Earth-facing surface is much lower than that on the zenith-facing surface. (Right) The meteoroid flux encountered by GOES-14: in this case, the flux is very similar on the nadir- and zenith-facing surfaces.

The online example library does not include detailed explanations of the coordinate systems used or outputs generated. Readers can refer to the MEM user guide for an explanation of MEM’s inputs and outputs as well as guidance on performing a MEM run [3]. A copy of the user guide is included in the MEM installation package and is readily [available online](#). The example library supplements, but is not a substitute for, the user guide.

By comparing sample environments, readers can view some of the ways in which meteoroid flux differs between trajectories. For instance, readers may notice that the Earth tends to protect one

continued on page 5

MEO Release

continued from page 4

side of spacecraft in low Earth orbit; the flux on the Earth-facing side of the *Aqua* trajectory is quite low compared to the flux on other surfaces (see Figure 2, left plot). This protective effect is not present for spacecraft at higher altitudes, such as *GOES-14* (right plot).

We have included two trajectories of current interest in our library: that of *JWST* and an NRHO, the planned orbit type for NASA's *Lunar Gateway*. However, users should not expect the library to cover every trajectory of note. The included examples are illustrative of the meteoroid environment, but they are not comprehensive.

Users might sometimes find that one of our example trajectories resembles an orbit they are considering for a mission. In such a case, they could potentially use one of our examples as a rough estimate of the environment their spacecraft will encounter; however, our examples should never be used for formal risk assessments. Any difference in trajectory or timing can result in a change in the meteoroid flux, and therefore a mission-specific trajectory should be used to assess and mitigate meteoroid impact risk.

More information on the example library, plus recommendations on trajectory sampling, are available in reference [8].

References

1. Moorhead, A., *et al.* "NASA's Meteoroid Engineering Model 3 and its ability to replicate spacecraft impact rates," *Journal of Spacecraft and Rockets*, vol. 57, issue 1, pp. 160-176, (2020).
2. Lear, D., *et al.* "Bumper: a tool for analyzing spacecraft micrometeoroid and orbital debris risk," *First International Orbital Debris Conference*, ntrs.nasa.gov/citations/20190022535.
3. Moorhead, A. "NASA Meteoroid Engineering Model (MEM) Version 3," NASA TM 2020220555, (2020).
4. Matney, M., *et al.* "The NASA Orbital Debris Engineering Model 3.1: Development, Verification, and Validation," *First International Orbital Debris Conference*, ntrs.nasa.gov/citations/20190033490.
5. Moorhead, A. and Matney, M. "The ratio of hazardous meteoroids to orbital debris in near-Earth space," *Advances in Space Research*, vol. 67, issue 1, pp. 384-392, (2021).
6. Lee, D. "Gateway Destination Orbit Model: A Continuous 15 Year NRHO Reference Trajectory," NASA white paper, ntrs.nasa.gov/citations/20190030294.
7. Moorhead, A., *et al.* "A two-population sporadic meteoroid bulk density distribution and its implications for environment models," *Monthly Notices of the Royal Astronomical Society*, vol. 472, issue 4, pp. 3833-3841, (2017).
8. Moorhead, A., *et al.* "A library of meteoroid environments encountered by spacecraft in the inner solar system," (submitted).

◆

Updated Flux Interpolation in ORDEM

A. MANIS AND P. ANZ-MEADOR

The NASA Orbital Debris Program Office (ODPO) develops the Orbital Debris Engineering Model (ORDEM) for use, in part, to determine risk from orbital debris to space missions. An important aspect of risk assessments is understanding the risk at specific critical sizes (diameters) of impactors, *i.e.*, those that could penetrate critical components. Since ORDEM outputs fluxes at 11 fiducial sizes in half-decade steps (log space) over the interval (10 μ m, 1 m), interpolation is necessary to calculate debris fluxes between these sizes.

Since version 3.0, ORDEM has included an interpolation scheme using the government off-the-shelf software embodied in the Piecewise Cubic Hermite Interpolating Polynomial (PCHIP) package, developed by the U.S. Department of Energy (DOE) Energy Science & Technology Software Center [1]. The PCHIP Fortran-language software has been implemented as code compatible with the ORDEM subroutine interface, licensed, and bundled with the ORDEM installer package. Several updates to the PCHIP implementation were introduced in ORDEM 3.1, addressing issues and concerns previously presented (ODQN vol. 22, issue 3, September 2018, pp. 8-9). These updates have been maintained in all subsequent versions of ORDEM, including the

current version 3.2. This project review summarizes key features of ORDEM's current PCHIP implementation. Further details and interpolation examples for specific test cases can be found in [2]; these cases may also be used by the debris community to verify PCHIP implementation in their custom software.

The PCHIP code and its component subroutines are predicated upon evaluating a piecewise cubic Hermite function at an array of points. All interpolations are conducted in $[\log_{10}(\text{size}), \log_{10}(\text{flux})]$ space. The presence of one or more zero values for flux is handled by abstracting zero as a number on the order of machine single-precision real values; in ORDEM, a value of 1×10^{-30} , or -30.0 in \log_{10} space, represents a zero-equivalent flux. After interpolation, interpolated flux values are converted from \log_{10} space back to linear space.

Figure 1 illustrates the critical function of PCHIP – interpolating a flux associated with a critical diameter – for ORDEM subpopulations. In this example, identical to the previous ODQN article for easy comparison, the 2019 flux on a spacecraft in an 841 \times 856 km altitude, 98.8° inclination orbit is portrayed by solid or open markers (11 reference points per subpopulation) and 500 points over 5 size decades were interpolated and are

continued on page 6

ORDEM Update

continued from page 5

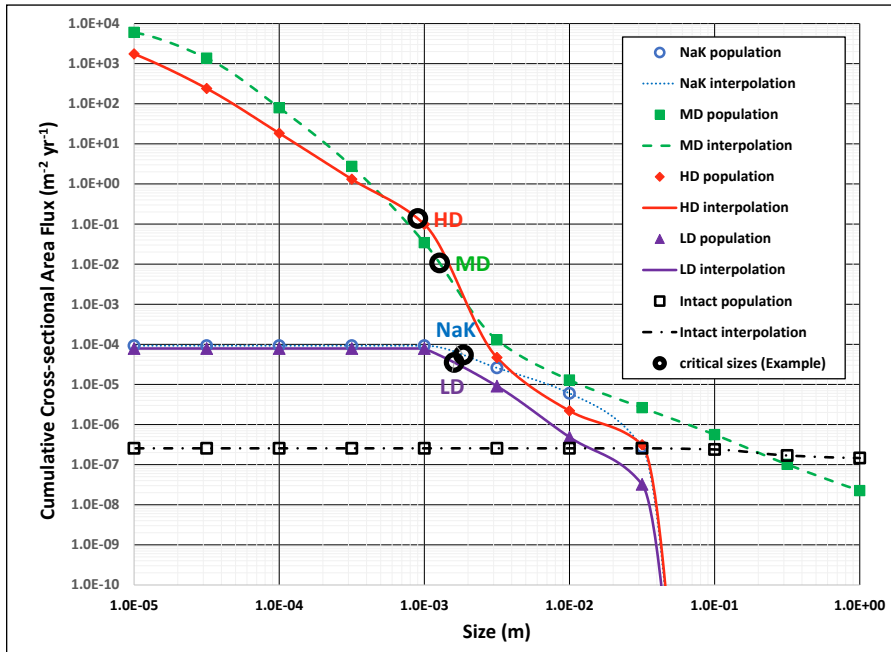


Figure 1. PCHIP interpolation of ORDEM 3.2 subpopulations for an 841 × 856 km altitude, 98.8° inclination orbit in 2019, with critical diameters required to penetrate an aluminum Whipple bumper indicated. Interpolation is necessary to assess the subpopulation flux at the computed critical diameters. Critical diameters vary according to the mass density of the debris projectile.

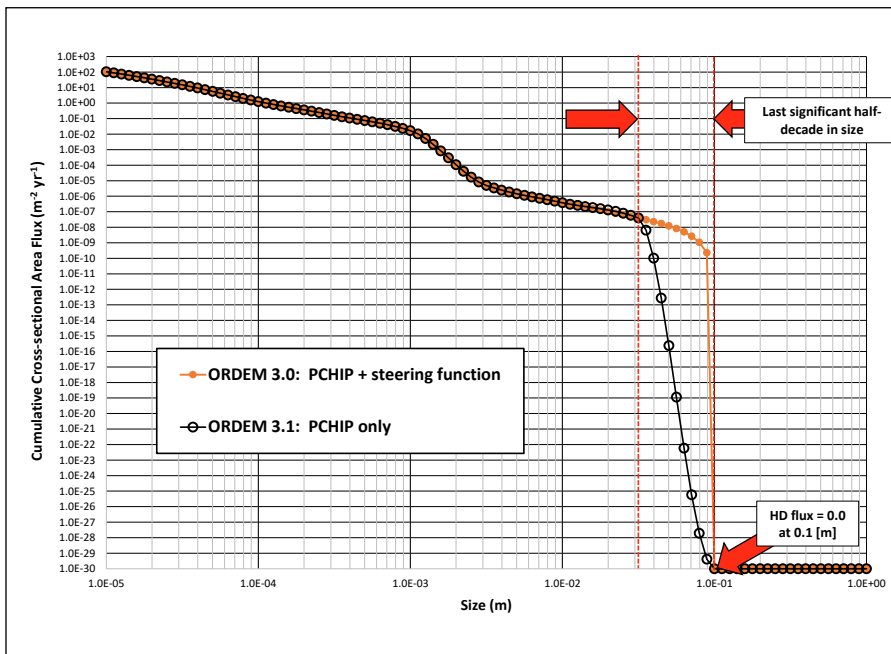


Figure 2. An example of interpolation with (ORDEM 3.0) and without (ORDEM 3.1) the steering function imposed on the last significant half-decade in size for the HD component of a typical ISS orbit in 2015.

represented in Figure 1 by solid or dotted lines. Critical diameters for penetration of a specific aluminum Whipple shield [3] configuration are indicated by heavy open circles for the low density (LD), medium density (MD), high density (HD), Sodium Potassium (NaK), and Intact populations. This set of five subpopulations is drawn from the ORDEM output IGLOOFLUX_SC.OUT file for a single case of azimuth, elevation, and relative velocity with respect to the target spacecraft. Note that critical diameters vary by the mass density attributed to each of the five subpopulations, but all critical diameters are located between two reference points, such that interpolation between these points is required to assess the subpopulation flux. For this evaluation, nominal mass densities of 0.9, 1.4, 2.8, 7.9, and 2.8 g/cm³ were used for the NaK, LD, MD, HD, and Intact families, respectively.

One important difference in ORDEM 3.1 interpolation, when compared to ORDEM 3.0, was the change in order of operations for interpolation and summation over the five ORDEM subpopulations. While ORDEM 3.0 summed the 5 ORDEM subpopulations at the 11 reference points and then interpolated, ORDEM 3.1 interpolates the fluxes for each subpopulation for a given azimuth, elevation, and relative velocity separately and then sums. This rectifies an inconsistency with NASA's Bumper 3 risk assessment code.

Another significant change in the PCHIP implementation for ORDEM 3.1 was in the handling of zero fluxes. For IGLOOFLUX_SC elements with non-zero cumulative flux F_i , one or more F_j may be zero. In this case, the last significant half-decade is defined as the last half-decade in size containing a non-zero flux; that is, the i -th half-decade in size with $F_i \neq 0.0$ and $F_{i+1} = 0.0$ (in linear space) is the last significant half-decade in size. In this case, F_{i+1} represents a significant zero and all F_j for $j > i + 1$ are considered non-significant. ORDEM 3.0 implemented a so-called "steering function," which introduced 8 additional points in (size, flux) space, for a total of 19 points, to handle the transition from a non-zero flux to a zero flux. In ORDEM 3.1, this steering function was removed, as it was determined PCHIP was robust enough to handle rapidly changing fluxes. Non-significant zero fluxes are ignored for the purpose of interpolation, so that interpolation is performed using the fluxes only up to and including the first significant zero.

continued on page 7

ORDEM Update

continued from page 6

The consequences of removing the steering function are illustrated in Figure 2. In this example, ORDEM 3.0 and ORDEM 3.1 results for a typical ISS orbit (400 × 400 km altitude, 51.6° inclination, random RAAN and argument of perigee) in 2015 are compared for an HD flux component of the IGLOOFLUX_SC.OUT output file. In this test case, the 0.0316 m to 0.1 m size interval constitutes the last significant half-decade; zero-flux reference points at 0.316 m and 1.0 m sizes are ignored for interpolation. As is evident, a potentially dramatic difference in outcomes can occur for the identical test case in the last significant half-decade, and the ORDEM 3.1 implementation (steering function omitted) can robustly interpolate between the last non-zero flux and the significant zero flux.

Behaviors unique to specific density families should also be noted, particularly for the LD family. There has been limited evidence found for LD debris in the Shuttle window and radiator cratering record. As a result, for a given bin in azimuth, elevation, and relative velocity in ORDEM, there may be a nonzero LD flux for sizes larger than 1 mm but no additional flux for smaller sizes. Therefore, the LD family has a hard cut-off at 1 mm, such that interpolation is only done over 1 mm and larger sizes (up to and including the last significant zero, if applicable).

The table summarizes the differences between the ORDEM 3.0 and ORDEM 3.1 (and subsequent) implementations. In summary, the ORDEM 3.1 implementation of the DOE PCHIP interpolation package simplifies implementation and obviates the necessity of significant pre-processing for post-ORDEM application programs such as the Bumper risk assessment code. Further, the order of operations in ORDEM 3.1 is now consistent with the community’s consensus order in Bumper.

Table. Differentiating features of the PCHIP interpolation routine in ORDEM 3.1 and later versions as compared to ORDEM 3.0.

ORDEM 3.0	ORDEM 3.1 and later
Employed quadratic “steering function,” a function of slope in penultimate half-decade.	“Steering function” deleted. Result: No pre-processing necessary for risk estimation codes.
Additional 8 points in (size, flux) space, for a total of 19 points, defined by the steering function in the last significant half-decade.	No additional points; PCHIP operates on ORDEM’s 11 (size, flux) reference points only, up to and including the last significant zero (when applicable). Result: No pre-processing necessary for risk estimation codes.
Flux from the five density families added, then interpolated to produce ORDEM’s SIZEFLUX_SC.OUT output flux.	Flux for each of the five density families interpolated, then added to produce ORDEM’s SIZEFLUX_SC.OUT flux. Result: ORDEM 3.1 is consistent with Bumper methodology and order of operations.

References

1. Fritsch, F.N., “PCHIP Final Specifications,” UCID-30194, Lawrence Livermore Laboratory under U.S. Department of Energy contract, August 1982.
2. Manis, A. *et al.*, “NASA Orbital Debris Engineering Model (ORDEM) 3.1: Model Process,” NASA/TP-20220004345, 2022.
3. Christiansen, E.L., “Shield Sizing and Response Equations,” NASA-TM-105527, 1991. ♦

Evolution of Major Debris Clouds in Low Earth Orbit

P. ANZ-MEADOR, A. KING, AND M. MATNEY

Low Earth orbit (LEO) is a dynamic environment due not only to the growth of human spaceflight and robotic missions but also the influences of geomagnetic storms and varying solar activity that change the atmospheric density at different altitudes. The natural environment, coupled with debris intrinsic properties such as ballistic coefficient, can significantly alter the medium- and long-term presence of debris clouds attributable to energetic breakup events. For these reasons, it is worthwhile to periodically review the evolution of major breakup events.

The NASA Orbital Debris Program Office (ODPO) provides an environmental overview and catalog of breakup and other debris-producing events to the community in the “History of On-orbit Satellite Fragmentations” [1]. In addition, the ODPO’s data-driven computer models require dedicated radar, optical, and *in-situ* measurements of the environment to understand

and characterize, in a statistically meaningful way, the historical evolution of fragmentation events for the purpose of modeling future behaviors and associated risk. This project review will examine major breakup events in the context of the current (01 June 2023) spatial density of the cataloged portion of their corresponding debris clouds as well as the temporal evolution and persistence of the cataloged debris from event epoch to date. The temporal evolution of the clouds through five critical LEO altitude bins will also be presented.

Table 1 presents selected breakup events in chronological order. Parent body orbital parameters are those at the time of the event.

These events comprise an accidental collision (Cosmos 2251 and Iridium 33), two deliberate direct-ascent antisatellite (ASAT) collisions (Fengyun 1C [FY-1C] and Cosmos 1408), and two explosions (NOAA 16 and the Yunhai 3’s CZ-6A rocket body).

continued on page 8

Debris Evolution

continued from page 7

Table 1. Significant breakup events considered in this review. Note (*) reference date is 01 June 2023

Satellite Name	International Designator	Satellite Catalog Number	Satellite Owner	Launch Date	Breakup Date	Cataloged to Date	Breakup Debris [*]		Parent Body	
							On Orbit	Apogee Altitude [km]	Perigee Altitude [km]	Inclination [°]
FENGYUN 1C	1999-025A	25730	PRC	10-May-99	11-Jan-07	3532	2747	865	845	98.6
COSMOS 2251	1993-036A	22675	CIS	16-Jun-93	10-Feb-09	1715	973	800	775	74.0
IRIDIUM 33	1997-051C	24946	USA	14-Sep-97	10-Feb-09	657	260	780	775	86.4
NOAA 16	2000-055A	26536	USA	21-Sep-00	25-Nov-15	458	447	858	842	98.9
COSMOS 1408	1982-092A	13552	CIS	16-Sep-82	15-Nov-21	1788	158	490	465	82.6
YUNHAI 3 CZ-6A R/B	2022-151B	54236	PRC	11-Nov-22	12-Nov-22	781	722	847	813	98.8

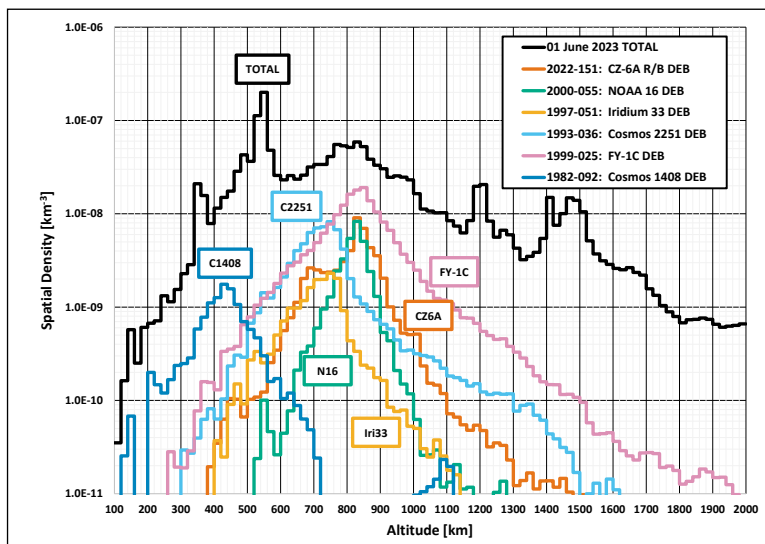


Figure 1. Total cataloged spatial density in LEO compared to the individual spatial density-altitude distributions of the six clouds examined.

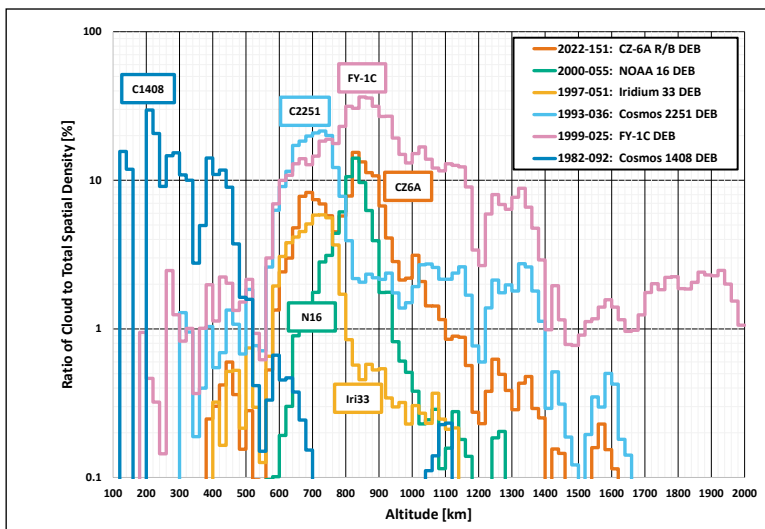


Figure 2. The ratio of individual cloud spatial density to the overall spatial density of cataloged objects within an altitude band. Epoch time is 01 June 2023.

Only the FY-1C, Cosmos 1408, and Cosmos 2251 events produced more cataloged debris to date than the fragmentation of the CZ-6A rocket body in November 2022. In the case of NOAA 16, only 5 other additional explosions produced more cataloged debris, and only one other event produced more than 400 [1]; however, these other event clouds are totally or mostly decayed from orbit or, in the singular case of the Cosmos 1275 cloud, does not significantly influence spatial density in the critical altitude bands considered herein. Thus, both explosion events included here would have been considered “major” events with long-term consequences absent the accidental and intentional collisions of the last two decades, with the CZ-6A rocket body being the single largest debris cloud in history under this scenario. In reality, the CZ-6A event is now the single largest debris cloud attributable to a rocket body. Figure 1 depicts the distribution in spatial density of the cataloged portion of these debris clouds with respect to each other and the total U.S. Satellite Catalog on 01 June 2023.

The readership should note that spatial density is a factor in the calculation of collision probability with another vehicle, but it does not account for other factors such as joint collision cross section and the relative speed and approach direction between the cloud background and the orbit of the other vehicle. Nonetheless, it is a useful metric for understanding relative risk, recognizing that both spatial density and the associated risk will be higher for objects that are uncataloged and smaller than the detection threshold for the Space Surveillance Network. Objects in and around the millimeter sizes present the highest mission-ending risk for spacecraft in LEO, thus characterizing the evolution of breakup clouds provides general insight into quantifying risk. While Figure 1 establishes the LEO perspective in an *absolute* sense, it is also useful to examine the *relative* contributions of each of the fragment clouds to the total environment. Figure 2 provides the ratio of these specific breakup events in relation to the background spatial density for cataloged objects.

continued on page 9

Debris Evolution

continued from page 8

Table 2. High value human spaceflight and robotic mission operational altitude bands (01 June 2023). Note Human Spaceflight (HSF) bands; the “A-Train” is the common nickname of the Afternoon Earth observer constellation. The colloquial “C-Train” acknowledges the first letter of the names of the Earth observing spacecraft resident in this slightly lower orbit.

Altitude Band Name	Altitude Band Range [km]	Noteworthy Residents	International Designator	Satellite Catalog Number	Satellite Owner(s)
HSF low	380-400	Chinese Space Station (CSS, <i>Tianhe-1</i>)	2021-035A	48274	PRC
HSF high	400-420	International Space Station (ISS)	1998-067A	25544	USA, Canada, ESA, Japan, CIS
HST	520-540	Hubble Space Station	1990-037B	20580	USA
“C-Train”	680-700	CloudSat, CALIPSO	2006-016A, B	29107, 29108	USA
“A-Train”	700-720	Aqua, Aura, OCO-2, GCOM-W1	Various	Various	USA, Japan

Over 10% of the spatial density within the altitude range of 400 km to 420 km is attributable to the Cosmos 1408 ASAT test at this epoch. Between 640 km to 760 km, the Cosmos 2251 debris contribute to an average of 20% of the spatial density population. Significantly, about 36% of the spatial density within the altitude range of 840 km to 860 km is due solely to the FY-1C ASAT test, providing the highest contributions to spatial density from 780 km to 2000 km when compared to these selected breakup events evaluated. Both the NOAA 16 and CZ-6A rocket body accidental explosions also contribute non-trivially, at approximately 15% each, at and around this altitude range.

Debris with perigees near the breakup altitude and much higher apogees can experience very long lifetimes and will continue to present a collision risk to active and derelict spacecraft and rocket bodies. For example, approximately 90% of FY-1C cloud ballistic coefficients (represented by the area-to-mass ratio, A/m) lie between 0.03 and 0.63 m^2/kg , with the distribution’s mode at 0.398 m^2/kg . If the debris is in a circular orbit at an altitude of 850 km on 01 June 2023, orbital lifetimes range from a decade to over a century, respective to the maximum and minimum A/m values quoted. However, if the debris is in a mildly elliptical orbit with perigee at 850 km altitude and apogee at 1700 km altitude, then lifetimes range from approximately 57 years to over a century, with a modal lifetime of approximately 91 years.

In lieu of a snapshot in epoch time over all LEO altitude bands, as shown in Figures 1 and 2, we may also examine the time history of cloud evolution through important altitudes; these altitudes, with specific attributes, are presented in Table 2.

The resident spacecraft occupied these bands as of 01 June 2023, though maneuvers and natural decay for spacecraft incapable of station keeping maneuvers mean that these spacecraft have occupied other or adjacent altitude

continued on page 10

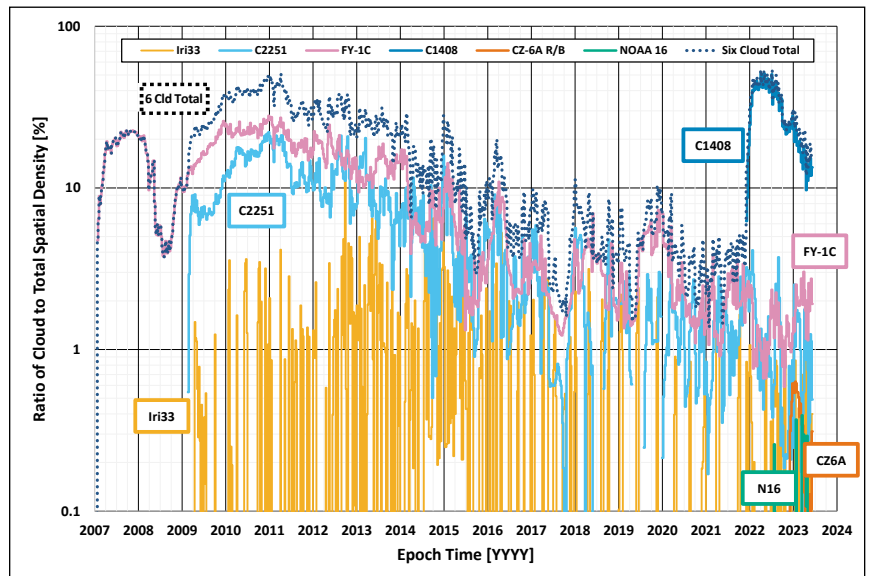


Figure 3. The time history of the cataloged component of the six debris clouds and cloud total experienced by the low HSF altitude band, currently occupied by the CSS.

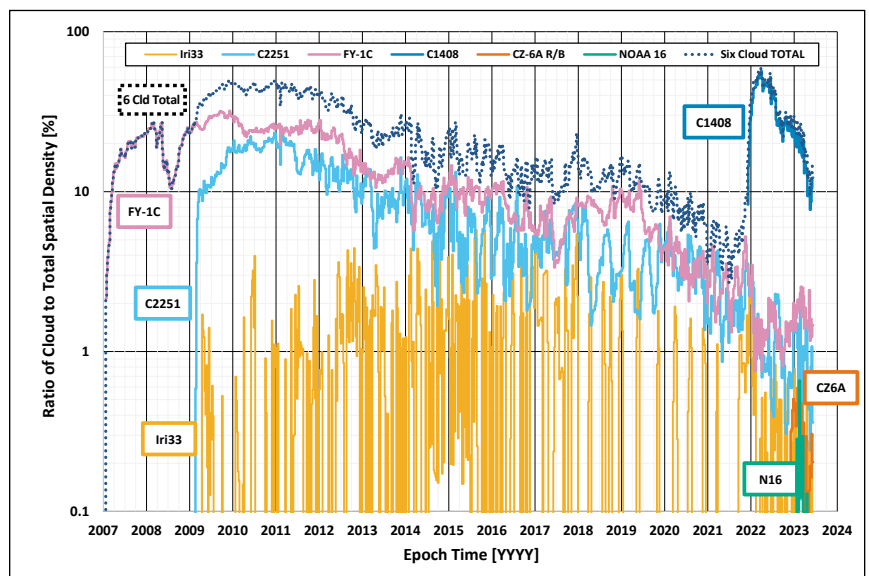


Figure 4. The time history of the cataloged component of the six debris clouds and cloud total experienced by the high HSF altitude band, currently occupied by the ISS.

Debris Evolution

continued from page 9

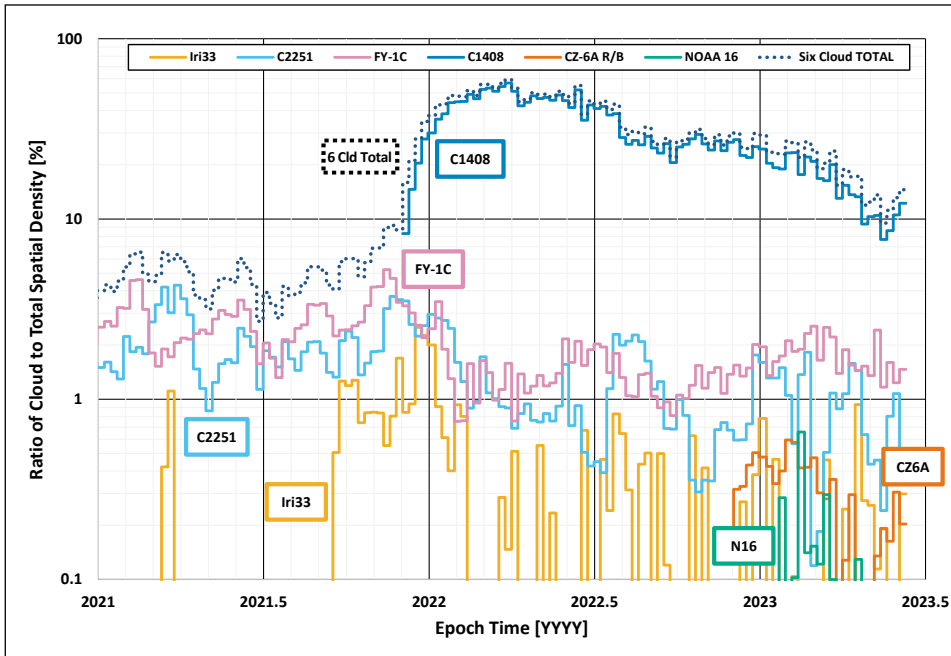


Figure 5. The time history of the cataloged component of the six debris clouds and cloud total experienced by the high HSF altitude band, currently occupied by the ISS. In this figure we consider only the time since 2021 to better view the effects of the Cosmos 1408 cloud on the ISS-local environment.

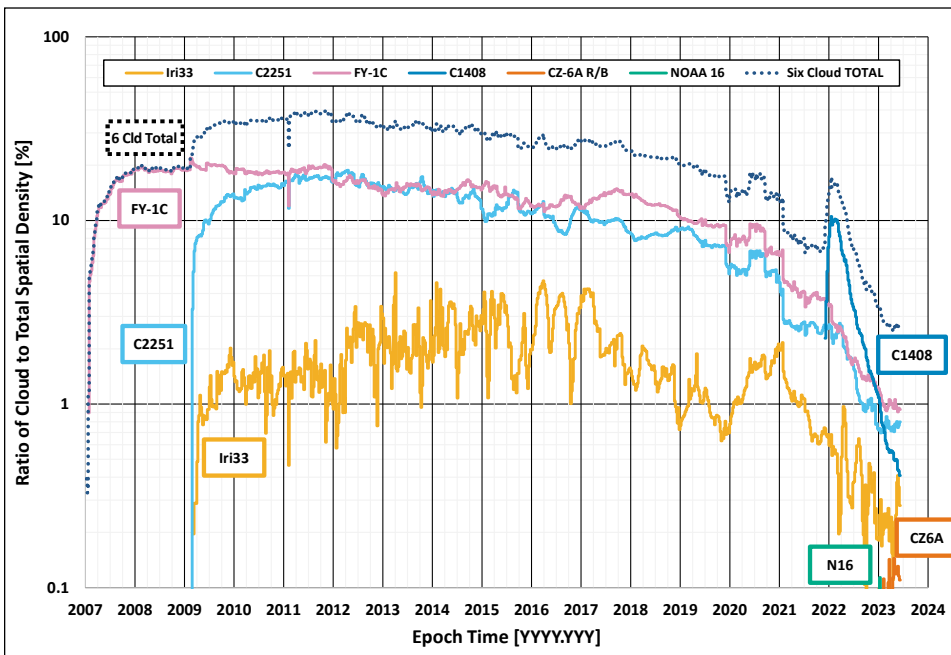


Figure 6. The time history of the cataloged component of the six debris clouds and cloud total experienced by the current HST altitude band.

bands in the past. For example, the ISS generally flies at an atmospheric density-constant altitude over the course of a Solar Cycle; at various times it has flown in both the HSF bands tabulated here. Descriptions in Table 2 are for illustrative purposes only over the debris clouds' life cycles to date.

Figures 3 and 4 present the very similar experiences of the low and high HSF bands. Figure 5 illustrates the recent experience of the ISS relative to the Cosmos 1408 ASAT event cloud.

The time histories of Figures 3 and 4 clearly depict that the adjacent altitude bins have experienced a similar cloud exposure with minor variations. Clearly evident are the short-term variations of the FY-1C and Cosmos 2251 clouds attributable to the influence of relatively few debris fragments in the lower reaches of these clouds. The Iridium 33 cloud, featuring generally larger values of the area-to-mass ratio, displays a lower spatial density and greater variation as fragments traverse the altitude band. Notable are the relatively small influences of the two explosions and, particularly visible in Figure 5, the pronounced effect of the Cosmos 1408 cloud due to its proximity to the HSF high band. Indeed, the ratio of Cosmos 1408 cloud spatial density to the individual FY-1C and other spatial densities peaked at approximately 36:1 in the first quarter of calendar year 2022. The Cosmos 1408 cloud accounted for approximately 20% of the daily warnings for satellite collisions in 2022 [2].

In contrast, Figure 6's time history at the HST altitude band displays essentially a steady state for the FY-1C and Cosmos 2251 clouds, as well as a significant contribution in local spatial density due to Cosmos 1408. The Iridium 33 cloud again displays significant variation as objects decay through the altitude.

Figures 7 and 8 depict an essentially steady state environment for FY-1C,

continued on page 11

Debris Evolution

continued from page 10

Cosmos 2251, and the Iridium 33 cloud – the latter with noticeably less variation due to the higher altitude. While present, the Cosmos 1408 cloud’s upper reaches represent less risk and are matched or exceeded by the relatively nearby explosions of NOAA 16 and the CZ-6A rocket body. In the former case, spatial density increases as fragments decay through the sun synchronous altitude bands employed by the C- and A-Train constellations.

In conclusion, six major debris generating events spanning the period 2007 to 2022 were examined to assess the influence of these evolving debris clouds to the overall risk profile of LEO, including but not limited to the unique international assets in typical HSF altitudes, the HST, and important sun-synchronous Earth observer constellation altitudes. It is apparent that even after up to 16 years post-event, breakup fragments in specific orbital regimes will continue to be problematic for the safekeeping of operational spacecraft from a collision warning and collision avoidance perspective, thus requiring continuous monitoring of the environment. The ODPO continues to utilize data from radar, optical, and *in-situ* measurements to develop and deploy environmental models and evolutionary models to assess the environment and support risk assessments from orbital debris to assets in Earth orbit. It is further evident that the implementation of domestic and international debris mitigation guidelines remains important in minimizing the generation of new fragmentation debris.

References

1. Anz-Meador, P., *et al.* “History of On-orbit Satellite Fragmentation, 16th Edition,” NASA/TP 20220019160 (December 2022).
2. Desuatels, E. “Space Security Issues,” Secure World Foundation 5th Summit for Space Sustainability, 13-14 June 2023. Accessed at <https://www.youtube.com/watch?v=N0UTB8mIYnM> 21 June 2023. ♦

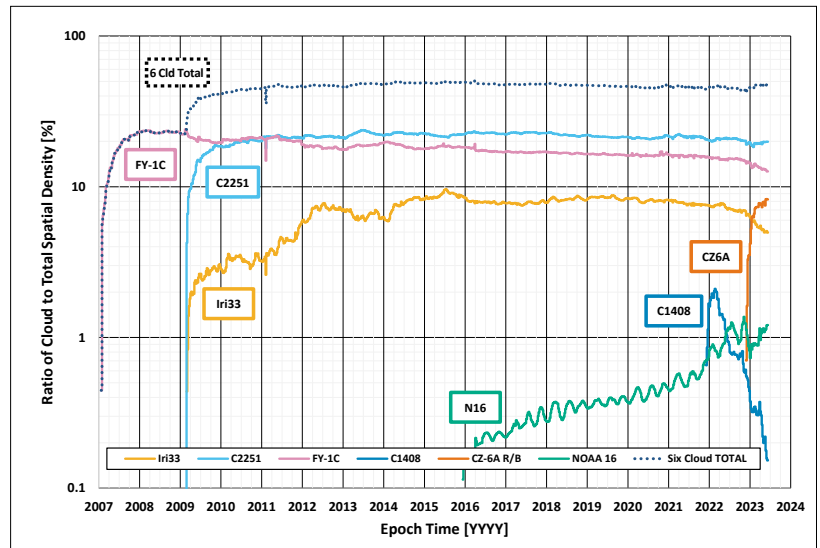


Figure 7. The time history of the cataloged component of the six debris clouds and cloud total experienced by the C-Train’s altitude band.

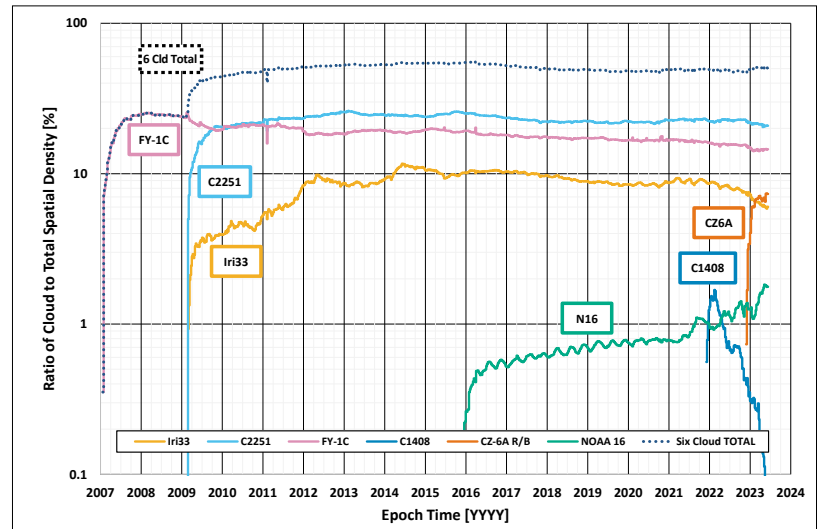
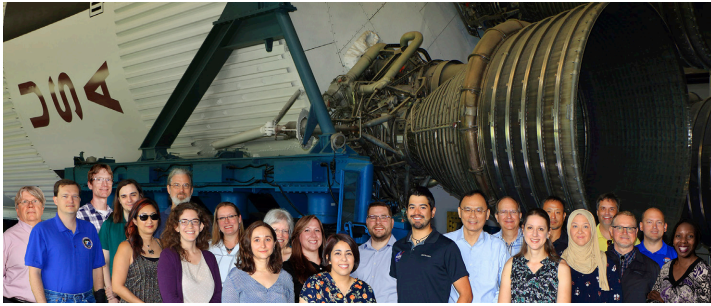


Figure 8. The time history of the cataloged component of the six debris clouds and cloud total experienced by the A-Train’s altitude band.

The ODPO announces an opening for a postdoctoral fellow via the [NASA Postdoctoral Program](#).

This position would support an *in-situ* sensor in development to characterize the small (millimeter-sized) orbital debris environment in low Earth orbit. Opportunities are available to support the development of the sensor and provide oversight and analyses that directly support future flight missions. For more information on this position, please see the [request](#).

ODPO Receives the 2022 Agency Group Achievement Honor Award



A number of ODPO members with the Saturn V rocket. L-R: Phillip Anz-Meador, Chris Ostrom, Matt Horstman, Austen King, Quanette Juarez, John Opiela, Ashley Johnson, Heather Cowardin, Jessica Arnold, Debi Shoots, Melissa Murray, Abigail Nguyen, James Murray, Corbin Cruz, Jer-Chyi Liou, Mark Matney, Alyssa Manis, Eun "Jay" Lee, Megan Ortiz, Brent Buckalew, John Seago, Andrew Vavrin, and Mechelle Brown. Several members who directly support the ODPO in its various efforts were not available for the photo.

The Chief and Deputy Chief of NASA's Office of Safety and Mission Assurance (OSMA) and the Director of OSMA's Mission Assurance Standards and Capabilities Division (MASCD) notified and congratulated the NASA Orbital Debris Program Office (ODPO) for its 2022 NASA Agency Honor Award/Group Achievement Award in April 2023. The ODPO was recognized "for exceptional contribution to monitor, assess, and mitigate risk from orbital debris to support the safe operations of human spaceflight and robotic missions." Dr. J.-C. Liou, NASA Chief Scientist for Orbital Debris and Program Manager for the ODPO, accepted the award on behalf of members of the ODPO during a ceremony held at Johnson Space Center on 16 May 2023.

Orbital debris is a major threat to human spaceflight and robotic missions in the near-Earth space environment. The ODPO has led the Agency to monitor orbital debris with measurement data collected by ground-based radars, optical telescopes, *in-situ* returned surfaces, and laboratory experiments for more than four decades.

continued on page 13

UPCOMING MEETINGS

19-22 September 2023: 24th Advanced Maui Optical and Space Surveillance Technologies Conference (AMOS), Maui, Hawaii, USA

The technical program of the 24th Advanced Maui Optical and Space Surveillance Technologies Conference (AMOS) will focus on subjects that are mission critical to space situational awareness. The technical sessions include papers and posters on orbital debris; space situational/space domain awareness; adaptive optics and imaging; astrodynamics; non-resolved object characterization; and related topics. The full program and information about the conference are available at <https://amostech.com>.

02-06 October 2023: 74th International Astronautical Congress (IAC), Baku, Azerbaijan

The IAC will convene in 2023 with a theme of "Global Challenges and Opportunities: Give Space a Chance." Of note, the 24th IAC was last held in Baku 50 years ago in 1973. The IAC's 21st International Academy of Astronautics Symposium on Space Debris will cover debris measurements and characterization; modeling; risk analysis; hypervelocity impact and protection; mitigation; post-mission disposal; space debris mitigation and removal; operations in the space debris environment; political and legal aspects of mitigation and removal; orbit determination and propagation; and financial gains with space debris. This year, the IAC will offer a venue for interactive presentations on space debris topics to allow more digital display capabilities for attendees. The program for the 2023 IAC is available online. Information about the conference and registration is available at <https://www.iafastro.org/events/iac/iac-2023/> and <http://iac2023.org/>.

09-13 October 2023: NASA Applied Space Environments Conferences (ASEC2023), Huntsville, Alabama, USA

The 2023 NASA Applied Space Environments Conferences (ASEC2023) will be held in Huntsville, Alabama. This conference provides a forum to discuss broad aspects of Earth's space environment with focused topics such as atomic oxygen; micro-meteoroids and orbital debris; radiation; spacecraft charging; space weather; anomalies and failures; current/future missions; in-flight observations; and instrument techniques. Abstract submission is now open. Additional details on abstract submission and registration can be found at <http://spaceweathersolutions.com/asec2023/>. ♦

ODPO Award

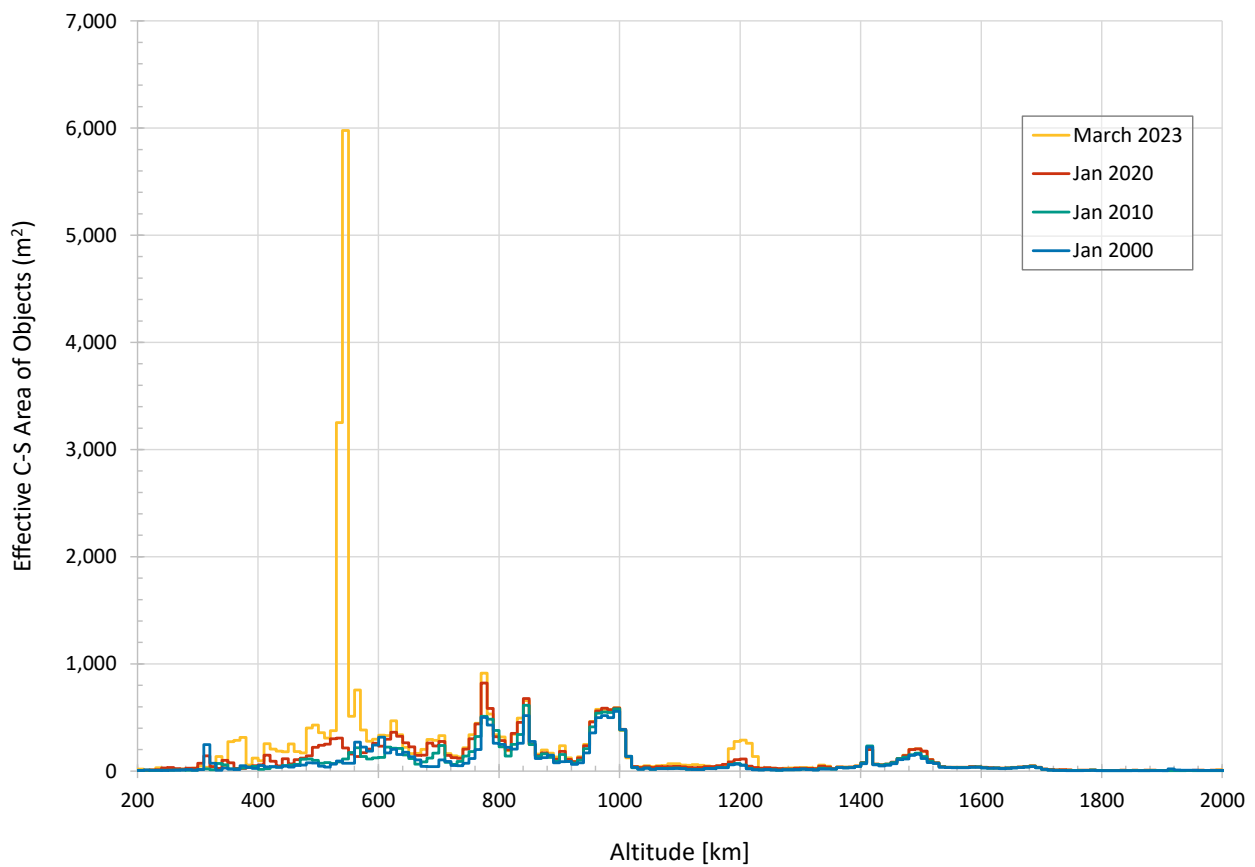
continued from page 12

The ODPO uses the measurement data to develop and update orbital debris models and mission support tools, such as the Orbital Debris Engineering Model (ORDEM) and Debris Assessment Software (DAS), two of the top-most requested software packages in the NASA Software Catalog. These tools are used by all NASA missions from low Earth orbit to geosynchronous orbit to assess risk from orbital debris and support the implementation of cost-effective protective measures for the safe operation of missions. The tools are also used by hundreds of operators (U.S., industry, international, etc.) from around the world for similar mission support and other applications.

The ODPO also leads efforts to develop and improve orbital debris mitigation best practices with the U.S. government, including the establishment of the U.S. Government Orbital Debris Mitigation Standard Practices (ODMSP) in 2001 and the recent update to the ODMSP in 2019. The ODPO also serves as the Agency lead in responding to new on-orbit fragmentation events and assessing risk to protect NASA human spaceflight and robotic missions. For example, following the anti-satellite (ASAT)

test on Cosmos 1408 conducted by the Russian Federation in November 2021, the ODPO worked closely with the ISS Program to assess the immediate risk to the ISS and supported the development of mitigation measures to protect the crew. The ODPO also reached out to the Department of Defense, the Massachusetts Institute of Technology Lincoln Laboratory, and the NASA Jet Propulsion Laboratory to collect special and timely radar measurement data on the ASAT fragments. Data from different sources were used to validate the initial risk assessments for the ISS and to support the update to ORDEM 3.2 and DAS 3.2.1 with the new ASAT fragment component. The two models were released to the space community in March 2022 to help the operators to assess and mitigate long-term risk from the ASAT fragments to better protect their missions.

The 2022 NASA Agency Honor Award/Group Achievement Award recognizes the ODPO's contributions to the Agency. As a Delegated Program in OSMA, the ODPO will continue to carry out its responsibilities to support NASA missions and serve the space community to address the orbital debris problem. ♦



Estimated effective average cross-sectional area of objects per 10 km altitude bin between 200 km and 2000 km altitude at four different epochs. These are objects, approximately 10 cm and larger, tracked by the Space Surveillance Network.

SATELLITE BOX SCORE

(as of 18 July 2023, cataloged by the U.S. SPACE SURVEILLANCE NETWORK)

Country/ Organization	Spacecraft*	Spent Rocket Bodies & Other Cataloged Debris	Total
CHINA	608	4415	5023
CIS	1569	5675	7244
ESA	98	29	127
FRANCE	88	536	624
INDIA	115	104	219
JAPAN	204	108	312
UK	692	1	693
USA	6529	5107	11636
OTHER	1186	84	1270
Total	11089	16059	27148

* active and defunct

Visit the NASA

Orbital Debris Program Office Website

<https://orbitaldebris.jsc.nasa.gov>

Technical Editor

Heather Cowardin, Ph.D.

Managing Editor

Ashley Johnson

Correspondence can be sent to:

Robert Margetta

robert.j.margetta@nasa.gov

or to:

Shaneequa Vereen

shaneequa.y.vereen@nasa.gov

National Aeronautics and Space Administration
Lyndon B. Johnson Space Center
 2101 NASA Parkway
 Houston, TX 77058



www.nasa.gov
<https://orbitaldebris.jsc.nasa.gov>

INTERNATIONAL SPACE MISSIONS

01 April 2023 – 30 June 2023

Intl.* Designator	Spacecraft	Country/ Organization	Perigee Alt. (KM)	Apogee Alt.(KM)	Incl. (DEG)	Addnl. SC	Earth Orbital R/B	Other Cat. Debris
1998-067	ISS dispensed objects	Various	413	419	51.6	6	0	6
2023-049A	OBJECT A	PRC	457	471	97.4	0	0	0
2023-050A	CHECKMATE 8	US	943	952	81.0	9	0	0
2023-051A	DUMMY MASS 3/SQX-1	PRC	281	436	97.3	0	0	0
2023-052A	INTELSAT 40E	ITSO	35778	35797	0.0	0	1	0
2023-053A	JUICE	ESA	EN ROUTE TO JUPITER			0	0	0
2023-054A	IMECE	TURK	669	678	98.2	47	0	0
2023-055A	FENGYUN 3G	PRC	403	414	50.0	0	1	0
2023-056A	STARLINK-30096	US	167	177	43.0	20	0	0
2023-057A	POEM 2	IND	586	619	9.9	0	0	0
2023-057B	LUMELITE 4	SING	574	585	10.0			
2023-057C	TELEOS 2	SING	578	579	10.0			
2023-058A	STARLINK-6038	US	561	565	97.7	45	0	4
2023-059A	O3BF04	SES	6426	8184	2.8	0	1	0
2023-059B	O3BF03	SES	5502	7672	3.5			
2023-060A	VIASAT 3	US	35786	35789	0.1	0	1	0
2023-060B	ARCTURUS	US	35781	35793	0.0			
2023-060C	GS-1	US	EN ROUTE TO GEO					
2023-061A	STARLINK-6156	US	558	560	43.0	55	0	4
2023-062A	TROPICS-05	US	537	550	32.7	0	2	0
2023-062C	TROPICS-06	US	530	550	32.7			
2023-063A	TIANZHOU 6	PRC	382	395	41.5	0	1	0
2023-064A	STARLINK-5990	US	567	571	70.0	50	0	4
2023-065A	STARLINK-5775	US	493	495	43.0	55	0	4
2023-066A	BEIDOU 3 G4	PRC	35757	35816	3	0	1	0
2023-067A	STARLINK-30122	US	522	524	43.0	21	0	0
2023-068A	ONEWEB-0561	UK	963	984	87.5	20	0	0
2023-069A	OBJECT A	PRC	452	494	41.0	0	1	4
2023-069B	OBJECT B	PRC	485	495	41.0			
2023-069C	OBJECT C	PRC	452	490	41.0			
2023-070A	AXIOM-2	US	412	420	51.6	0	0	1
2023-071A	PROGRESS MS-23	CIS	417	418	51.6	0	1	0
2023-072A	NEXTSAT-2	SKOR	537	551	97.54	7	0	0
2023-073B	TROPICS-03	US	537	552	32.7	0	2	0
2023-073C	TROPICS-07	US	531	551	32.7			
2023-074A	COSMOS 2569	CIS	508	510	97.4	0	0	0
2023-075A	ARABSAT 7B (BADR 8)	AB	EN ROUTE TO GEO			0	1	0
2023-076A	NVS-01	IND	EN ROUTE TO GEO			0	1	0
2023-077A	SZ-16	PRC	382	395	41.5	0	1	4
2023-078A	STARLINK-6197	US	462	467	70	51	0	4
2023-079A	STARLINK-30119	US	522	524	43.0	21	0	0
2023-080A	DRAGON CRS-28	US	253	404	51.6	0	0	1
2023-081A	OBJECT A	TBD	491	514	97.4	25	1	0
2023-082A	LONGJIANG 3	PRC	488	497	49.1	0	1	0
2023-083A	STARLINK-6206	US	450	451	43.0	51	0	4
2023-084A	OBJECT A	TBD	519	532	97.5	69*	0	0
2023-085A	OBJECT A	PRC	533	550	97.5	40	0	0
2023-086A	NUSANTARA TIGA	INDO	EN ROUTE TO GEO			0	0	0
2023-087A	SHIYAN 25 (SY-25)	PRC	293	313	96.6	0	0	0
2023-088A	STARLINK-5847	US	371	373	43.0	46	0	4
2023-089A	USA 345	US	NO ELEMS. AVAILABLE			0	1	0
2023-090A	STARLINK-6132	US	364	366	43.0	55	0	4
2023-091A	METEOR M2-3	CIS	809	816	98.8	**		

* Incomplete cataloging/identification